Optimum electromagnetic energy converters[‡]

O. Papes[*,†], R. Peikert, J. Biela and J. Hugel

Department of Mechanical and Process Engineering, Institute of Mechanical Systems, ETH Zurich, CH-8092 Zurich, Switzerland

SUMMARY

This paper investigates the optimal shape of electromagnetic devices in terms of volume. An entangled pair of a coil and a core is considered. The dimensionless volume characteristic z_V of this transformer design is defined, which is a measure for the volumetric efficiency of electromagnetic devices. The description of the design is considerably simplified using symmetry arguments. Based on electromagnetic laws, a mapping between the contours of the core and the coil is found. Consequently, the volume characteristic is expressed in terms of the core contour only. The core contour is then discretized using Bézier segments and Fourier modes, and the minimization of the volume characteristic is carried out numerically. While previous engineering efforts brought down z_V to approximately 11.6, this paper presents an optimized transformer design characterized by $z_V = 10.07365 \pm 10^{-5}$. To the best of the authors' knowledge, this is the most efficient shape of a simple coil-core assembly in terms of volume published up to now. Copyright © 2009 John Wiley & Sons, Ltd.

1. INTRODUCTION

Electromagnetic energy conversion is based on Ampère's and Faraday's laws, which are parts of Maxwell's equations for the electromagnetic fields [1]. In nearly all practical applications as are transformers, inductors, generators or motors, the electric field is guided by copper wires and the magnetic field by an iron (ferrite) core. These two geometrically defined channels for the electric current and the magnetic flux are linked together like two chain links, cf. Figure 1. Both, the current and the flux, are limited by saturation effects in the iron and the admissible heat production in the core and the windings. It is the task of the designer to find under these limitations a good geometry which is an optimum with respect to volume and weight [2], mechanical stresses [3], transmitted power and losses [4], flux linkage [5], costs [6], or any other cost function of interest. Depending on this choice and the kind of device, the designs will differ. One of the simplest electromagnetic energy converters is the transformer and its volume is the basic quantity for many other parameters subject to optimization. For example, if the volumes occupied by the iron core and the windings are multiplied by the specific weights of the corresponding materials, the optimization procedure will lead to the minimum weight.

In the following, some idealizations and assumptions are introduced to define the task of minimizing the volume for a given power, which is the problem considered in this paper. A number of physical effects as are radiation, flux leakage, resistance, heat production, dissipation, structure elasticity, and mechanical stress are neglected since this would impose additional constraints and introduce new parameters, thus making the optimization more difficult and the result less transparent. Concerning engineering aspects, simplifying assumptions on the topology of core and windings are introduced, thus allowing to speak about characteristic areas of cross sections and mean lengths of the corresponding channels. A simplified picture for the magnetic field in the core and the electric current in the windings is used. No division in primary and secondary circuit is considered in the windings.

It is assumed that the magnetic flux density norm B in the core and the current density norm J in the windings achieve the allowed maximum everywhere and thus are spatially constant. So, the cross sections A_1 of the core and A_2 of the windings must have constant

---

*Correspondence to: O. Papes, Department of Mechanical and Process Engineering, Institute of Mechanical Systems, ETH Zurich, CH-8092 Zurich, Switzerland.
†E-mail: ondrej.papes@imes.mavt.ethz.ch
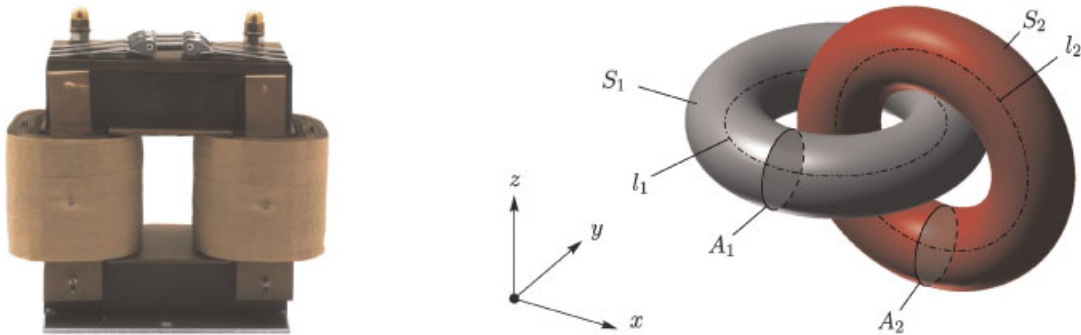
Figure 1. Left: high voltage transformer (Fa. Wickeltechnik Langer, Germany). Right: simple representation of a transformer by two enclosing solid bodies—the roles of the core S_1 and the windings S_2 can be exchanged.

values in order to conserve the total magnetic flux $\Phi = B \cdot A_1$ and the total current $I = J \cdot A_2$, cf. Figure 1. With the mean lengths l_1 for the core and l_2 for the windings, the total volume V and transferred power P of the transformer [2] become:

$$V = l_1 \cdot A_1 + l_2 \cdot A_2 \tag{1}$$

$$P = \frac{k \, \omega J \, B}{2\sqrt{2}} \cdot A_1 \cdot A_2 \tag{2}$$

ω is the angular frequency and the factor $k \in [0, 1]$ is the overall utilization, both are constants with respect to the following optimization. Thus, an optimum device is obtained, if for a fixed volume V the power P is maximized, or vice versa, if for a fixed power the volume is minimized.

From the equations above, the law for scaling electromagnetic devices is apparent. The transferred power grows with the fourth power of the length (without considering thermal limitations) and the volume only with the third power, so in large units the material is used more economically than in small ones. To get rid of this influence when searching for an optimum design, the volume characteristic

$$z_V = \frac{V}{(A_1 \cdot A_2)^{3/4}} \tag{3}$$

is defined, which is a dimensionless ratio of volume and power and should be minimized when searching for the optimal geometry. The number z_V is a characteristic figure for geometrically similar designs and it is a simple task to calculate it for a given construction. A more detailed assessment—not presented here—shows that the minimum value for the volume characteristic must lie within the limits $4\sqrt{\pi} < z_V < 8\sqrt{\pi}$, where the upper bound was first addressed in Reference [2]. The task now is to find the minimum value for z_V and the shapes of the core and the windings of a transformer with this characteristic value. The problem is symmetrical in the following sense: if an optimal pair of shapes for the core and the windings is found, the roles of core and windings can be interchanged and a dual solution is obtained.

Mathematically speaking, the search for the minimum z_V is a problem best approached within the framework of the calculus of variations [7]. Many classical problems, for instance to find the sphere as the shape which maximizes volume for a given surface area, were solved with this approach analytically. But for the transformer problem with its two linked solids no simple solution can be expected. The dependencies between the areas A_1, A_2 and the mean lengths l_1, l_2 in Equation (1) can be quite complicated. Nevertheless, the optimum shapes and the minimum z_V were found recently and are discussed in the following.

Independent from the intellectual challenge, the question may come up, how relevant for the practical engineering and design work these discussions and results are. The optimum characteristic z_V for the volume or z_W for the weight are indicators, how far away a practical design is from the optimum and thus bear a similar meaning as the Carnot-efficiency in thermodynamics. In the past, as will be shown, the electrical engineers have done their work quite well. In Figure 2, the transformer from a locomotive of the Rhaethian Railways in Switzerland is shown. This is a narrow-gauge system, designed for operation in the mountains, so very
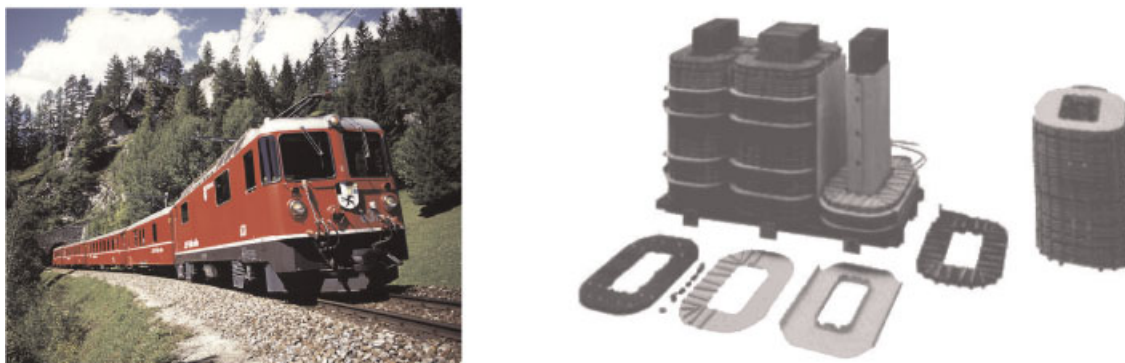
Figure 2. Left: the narrow-gauge locomotive Ge 4/4 II of the Rhaetian Railways RhB, Switzerland (photography by Philipp Glitzner, Austria). Right: the inbuilt transformer realizes $z_V \approx 11.6$ (ABB Sécheron SA Genève).

powerful locomotives are essential; however, the volume is very limited. With this type of construction the volume characteristic was brought down to $z_V \approx 11.6$ and this figure is not too far from the absolute minimum derived in the following.

The paper is organized as follows. The optimization problem is defined and solved in Section 2. In Section 2.1, all assumptions and simplifications are listed and arguments for the postulated topological properties and geometrical symmetries of the considered designs are given. Based on these assumptions the mathematical definition of the constrained optimization problem is introduced in Section 2.2. In Section 2.3 an exact mathematical relation between the shapes of core and windings is found and is recast into an efficient algorithm in Section 2.4. Two different discretizations of the geometry are introduced in Section 2.5. The minimization of z_V is demonstrated in Section 2.6, where four numerical solution strategies are compared and are demonstrated to gain consistent results that are identical up to the sixth significant digit of z_V. The paper closes with concluding remarks in Section 3.

2. MINIMIZATION OF THE VOLUME CHARACTERISTIC

2.1. Simplifications and reduction of dimensionality

A transformer basically consists of two 3D solids, cf. Figure 1: a core made of magnetically conductive material (solid S_1, gray) and the windings made of electrically conductive material (solid S_2, red), which enclose each other. Starting with this simple picture of a prototypic construction, steps toward an optimized design which minimizes the characteristic z_V make it necessary to rearrange the geometry. However, all optimizing processes must be carried out in such a way that the feasibility of the construction is guaranteed:

- The two solids S_1 and S_2 must not intersect;
- They must allow for the accommodation of physically possible and functionally reasonable current and magnetic fields; and
- These two fields have to be properly entangled in order to ensure the functionality of the transformer.

So the optimization is subject to several interrelated constraints and the problem is fully 3D. As a fully 3D optimization is beyond the scope of this report, some plausible assumptions are introduced which considerably simplify the problem, all assumptions are listed in Table I.

In the following, a justification for the symmetry assumptions is given and the 3D optimization problem is demonstrated to reduce to a 2D formulation. Starting with the situation depicted in Figure 1 but allowing for free cross section shapes and paths, a first way

Table I. List of assumptions used for the setup of the optimization problem.

Construction:	Ring transformer design, consisting of an entangled pair of core and windings in tight contact
Neglected:	Radiation, flux leakage, resistance, heat production, dissipation, structure elasticity, mechanical stress
Core:	Torus-like with free cross section shape but constant cross section area A_1, the magnetic flux density is of constant magnitude B and orthogonal to cross section
Windings:	Assembled from infinitesimal tori entangling the core torus, free cross section shape but constant total cross section area A_2, the current density is of constant magnitude J and orthogonal to cross section
Symmetries:	Cylindrical and reflection symmetry
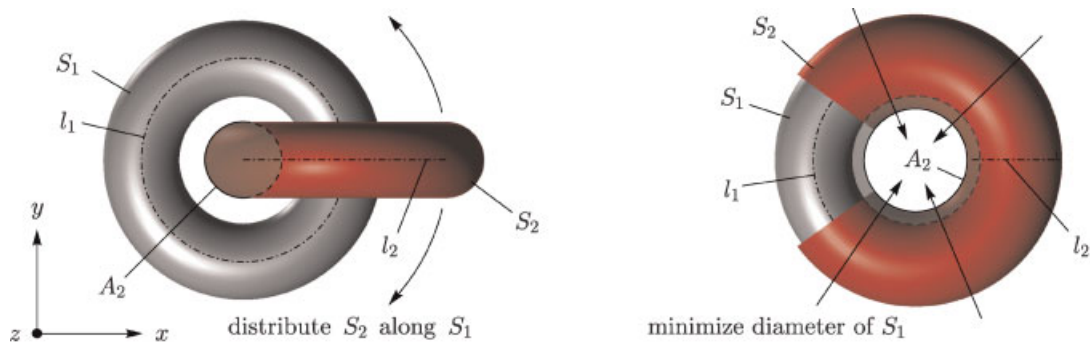
Figure 3. First plausible adjustments reducing the volume characteristic.

of optimizing z_V is to search for designs where the total volume $V = V_1 + V_2$ is minimized through various shape variations while keeping the areas A_1 and A_2 constant. Further optimization steps involve the identification of possible symmetries and the optimization of particular cross section shapes of the core.

2.1.1.   Ad hoc minimization of the volume.   Recalling the necessary constancy of the cross sections A_1 and A_2 and Equation (1), the volume becomes minimal if the mean lengths l_1 and l_2 are minimized. In the considered case, the mean length l_2 is minimized by distributing the solid S_2 uniformly along the circumference of S_1 and in tight contact with S_1, cf. Figure 3 left. Furthermore, l_1 is minimized by radially shrinking the setup until the central opening is completely occupied by solid S_2, cf. Figure 3 right. Note that due to constancy of A_2 the shape of this area will differ at different distances from the center.

So far, the transformer design was rearranged such that the areas A_1 and A_2 were kept constant and the path lengths l_1 and l_2 were minimized. However, this does not yet determine the shapes of neither the paths nor the cross-sections, in principle the shapes could change along the corresponding paths. Nevertheless, intuition suggests that it should be admissible to subject the overall design to symmetries, i.e., cylindrical and reflection symmetry as anticipated in Figure 3. On the one hand, invoking such geometrical symmetries substantially simplifies the optimization process since the number and complexity of considered designs are reduced. On the other hand, assuming the existence of symmetries restricts the set of designs and hence there is a risk of excluding the best design from the optimization. Thus, it is necessary to justify symmetries, for instance by showing that within a large set of designs the optimum z_V is realized by a symmetric design.

2.1.2.   A method for justifying symmetries.   The following simple, set theoretical concept is applied to show the plausibility of symmetries. Imagine a set $\mathcal{T}$ of transformer designs. The subset $\mathcal{T}_S \subset \mathcal{T}$ consists of designs which have a particular symmetry $\mathcal{S}$ and the complementary set $\mathcal{T}_N = \mathcal{T} \backslash \mathcal{T}_S$ consequently consists of designs which lack this symmetry. Now find a rule $\mathcal{R} : \mathcal{T}_N \rightarrow \mathcal{T}_S$ which assigns to each nonsymmetric design $\mathcal{D}_N \in \mathcal{T}_N$ a symmetric design $\mathcal{D}_S = \mathcal{R}(\mathcal{D}_N) \in \mathcal{T}_S$ such that the volume characteristic is retained or becomes better according to $z_V(\mathcal{D}_S) \leq z_V(\mathcal{D}_N)$. If such a rule $\mathcal{R}$ exists, then we know there is no unsymmetric design in $\mathcal{T}_N$ which couldn't be replaced or outperformed by some symmetric design in $\mathcal{T}_S$. Thus, we are allowed to search for the optimum design in $\mathcal{T}_S$ and can disregard the geometrically more complicated subset $\mathcal{T}_N$. Formally this reads as:

$$\forall \, \mathcal{D}_N \in \mathcal{T}_N \, \exists \, \mathcal{D}_S = \mathcal{R}(\mathcal{D}_N) \in \mathcal{T}_S \mid z_V(\mathcal{D}_S) \leq z_V(\mathcal{D}_N)$$
$$\Longrightarrow \min_{\mathcal{T}} \, z_V = \min_{\mathcal{T}_S} \, z_V \tag{4}$$

The difficulty is to construct for any investigated symmetry $\mathcal{S}$ appropriate pairs of sets $\mathcal{T}$ and rules $\mathcal{R}$. The sets $\mathcal{T}$ should be as large as possible to make the statement most general. However, for too large sets typically no rules $\mathcal{R}$ can be found anymore. Thus, the here presented arguments for the necessity of symmetries are valid under the restriction that concurring geometries stem from special sets which allow for the construction of a rule.

2.1.3.   Cylindrical symmetry.   The cylindrical symmetry $\mathcal{S}$ is characterized by a z-axis and a cylindrically symmetric design $\mathcal{D}_S$ is invariant under rotations by an arbitrary angle around this axis. The set $\mathcal{T}$ is constructed such that it consists of designs which result
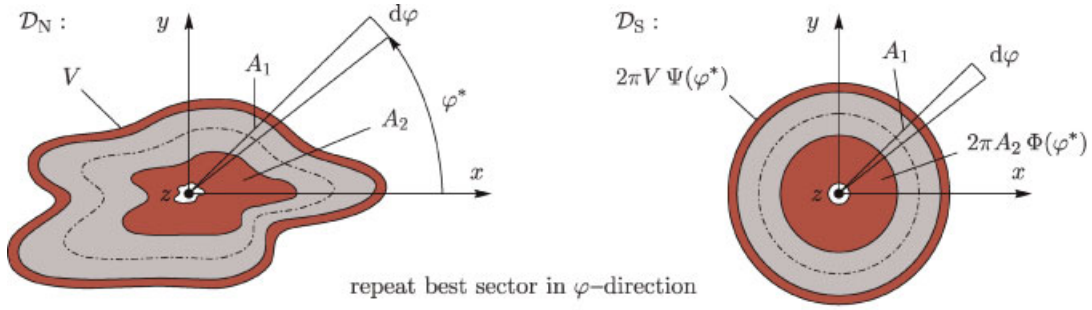
Figure 4. The argument for a cylindrically symmetric transformer design.

from finite geometrical perturbations of initially cylindrically symmetric constructions, cf. Figure 4. By definition, all nonsymmetric designs $\mathcal{D}_N \in \mathcal{T}_N$ must have the following properties:

1. Every $\mathcal{D}_N$ must be decomposable into infinitesimal, sector-like slices and every such slice is suitable as the infinitesimal generator for a new, cylindrically symmetric $\mathcal{D}_S$.
2. The shape and size of the slices of $\mathcal{D}_N$ might vary in the circumferential direction, but all slices must have the same area A_1.
3. A slice located at angle φ contributes to the total area A_2 and the total volume V of $\mathcal{D}_N$ with the differentials $A_2\Phi(\varphi)\mathrm{d}\varphi$ and $V\Psi(\varphi)\mathrm{d}\varphi$, respectively. $\Phi(\varphi)$ and $\Psi(\varphi)$ are two positive and 2π-periodic functions which integrate to 1 over the interval $[0, 2\pi]$.
4. At least one sector at a specific angle $\varphi^* \in [0, 2\pi]$ must exist for which holds $\sqrt[4]{2\pi}\Psi(\varphi^*)/\Phi(\varphi^*)^{3/4} \leq 1$.

A good rule $\mathcal{R} : \mathcal{T}_N \rightarrow \mathcal{T}_S$ is now obtained by assigning to $\mathcal{D}_N$ the one $\mathcal{D}_S$ which results from the revolution of the φ^*-sector in the circumferential direction. According to postulates 2 and 3, the volume characteristic of the parent design $z_V(\mathcal{D}_N)$ and an upper bound[1] for the volume characteristic of the derived symmetric design $z_V(\mathcal{D}_S)$ are:

$$
z_V(\mathcal{D}_N) = \frac{V}{(A_1 \cdot A_2)^{3/4}} \cdot \frac{\int_0^{2\pi} \Psi(\varphi)\,\mathrm{d}\varphi}{\left(\int_0^{2\pi} \Phi(\varphi)\,\mathrm{d}\varphi\right)^{3/4}} = \frac{V}{(A_1 \cdot A_2)^{3/4}}
$$

$$
z_V(\mathcal{D}_S) \leq \frac{V}{(A_1 \cdot A_2)^{3/4}} \cdot \frac{\int_0^{2\pi} \Psi(\varphi^*)\,\mathrm{d}\varphi}{\left(\int_0^{2\pi} \Phi(\varphi^*)\,\mathrm{d}\varphi\right)^{3/4}} = z_V(\mathcal{D}_N) \cdot \frac{\sqrt[4]{2\pi}\Psi(\varphi^*)}{\Phi(\varphi^*)^{3/4}}
$$

(5)

By comparing Equation (5) with postulate 4., we immediately see that the rule $\mathcal{R}$ indeed fulfills $z_V(\mathcal{D}_S) \leq z_V(\mathcal{D}_N)$. Invoking the cylindrical symmetry therefore is an adequate way for minimizing z_V in the set $\mathcal{T}$. It remains to be discussed whether the above constructed set $\mathcal{T}$ is not too special. From all four postulates, the most special one is the fourth requiring the existence of a specific sector. It can be shown that dropping this property generates a comparably small but nevertheless existing set of counterexamples, for which symmetrization in the sense of $\mathcal{R}$ leads to an increase of z_V and so destroys the symmetry argument.

The interested reader may countercheck this by considering a design characterized by $\Phi(\varphi) = \frac{1}{2\pi} + \varepsilon\,\mathrm{sig}(\sin(\varphi))$ and $\Psi(\varphi) = \frac{1}{2\pi} + \frac{3}{4}\varepsilon\,\mathrm{sig}(\sin(\varphi))$, where $\varepsilon \in \left(0, \frac{1}{2\pi}\right)$ is a perturbation parameter and sig(.) is the signum function fulfilling $\mathrm{sig}(x) = 1$ for $x \geq 0$ and $\mathrm{sig}(x) = -1$ for $x < 0$. A Taylor series expansion of the crucial term gives $\sqrt[4]{2\pi}\Psi(\varphi)/\Phi(\varphi)^{3/4} = 1 + \frac{3\pi^2}{8}\varepsilon^2 + \ldots$ for any angle φ and comparing this outcome with Equation (5), it is clear that symmetrization will increase z_V instead of lowering it. Such counterexamples, although physically admissible, are excluded by postulate 4. From a randomly generated set of nonsymmetric designs $\mathcal{D}_N$ with reasonable fluctuations in the functions $\Phi(\varphi)$ and $\Psi(\varphi)$, only a very small fraction is affected by this postulate and so the argument for cylindrical symmetry presented here is stronger than the definition of $\mathcal{T}$ might suggest. On these grounds, the optimum design is assumed to have the cylindrical symmetry.

---

[1] By going from $\mathcal{D}_N$ to $\mathcal{D}_S$, additionally the effective cross-section A_1 may increase and z_V decrease if the magnetic lines are reoriented into the circumferential direction.
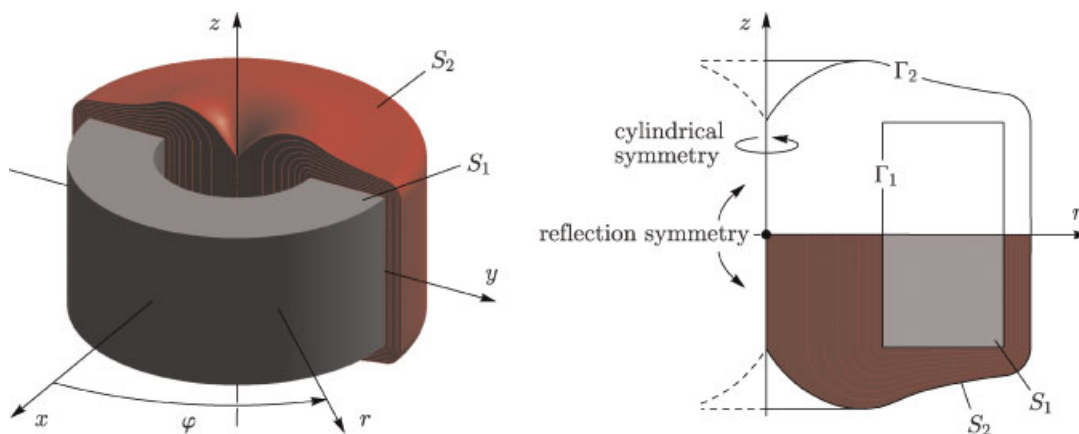
Figure 5. A possible reflection symmetric design with a rectangular core.

2.1.4. Reflection symmetry. The reflection symmetry $\mathcal{S}$ is characterized by a *xy*-plane being perpendicular to the aforementioned *z*-axis and a reflection symmetric design $\mathcal{D}_S$ is invariant under mirroring along this plane. The set $\mathcal{T}$ is constructed such that it consists of cylindrically symmetric designs in the sense of Section 2.1.3, cf. Figure 5. By definition, all designs $\mathcal{D}_N \in \mathcal{T}_N$ lacking the reflection symmetry must have the following properties:

1. The *xy*-plane cuts the $\mathcal{D}_N$ into two parts, one above and the other below the plane. Upon being reflected, both parts can generate a new, reflection symmetric $\mathcal{D}_S$.
2. Both parts have the same area A_2 and the same volume $V/2$, where A_2 and V are the windings cross-section and volume of $\mathcal{D}_N$, respectively.
3. The *xy*-plane cuts the core cross-section A_1 of $\mathcal{D}_N$ into two not necessarily equal areas $A_1\Phi$ above and $A_1(1-\Phi)$ below the plane, $\Phi \in (0,1)$.

The rule $\mathcal{R} : \mathcal{T}_N \to \mathcal{T}_S$ is constructed such, that the part of $\mathcal{D}_N$ which maximizes the A_1-fraction $\Psi = \max\{\Phi, 1 - \Phi\} \in \left[\frac{1}{2}, 1\right)$ is mirrored. The so obtained $\mathcal{D}_S$ has the volume characteristic:

$$z_V(\mathcal{D}_S) = \frac{V}{(2\Psi A_1 \cdot A_2)^{3/4}} = z_V(\mathcal{D}_N) \cdot (2\Psi)^{-3/4} \tag{6}$$

Since $(2\Psi)^{-3/4} \leq 1$ holds for $\Psi \in \left[\frac{1}{2}, 1\right)$, the rule $\mathcal{R}$ fulfills $z_V(\mathcal{D}_S) \leq z_V(\mathcal{D}_N)$ and the assumption of reflexion symmetry is admissible. Therefore, if searching for the global minimum of z_V, it is sufficient to consider designs which have both, cylindrical and reflection symmetry. The considered transformer geometry is obtained from the revolution of a single representative slice around the *z*-axis and this slice is in addition reflection symmetric. Thus, the dimensionality of the initially complicated 3D problem was reduced to 2D, cf. Figure 5.

In the following, only the representative slice will be investigated. The slice is characterized by the contour Γ_1 of the core and the outer contour Γ_2 of the windings in the first quadrant of the *rz*-plane. Consequently, only nonnegative values of *r* and *z* are considered. The two contours must satisfy certain conditions in order to describe a feasible transformer geometry:

- The two curves Γ_1 and Γ_2 lie in the first quadrant of the *rz*-plane;
- They are continuous and assumed piecewise continuously differentiable;
- They begin and finish on the *r*-axis, in addition Γ_2 starts on the *z*-axis, and they do not intersect;
- Γ_2 lies outside the region enclosed by Γ_1 and the *r*-axis; and
- The "distance" between Γ_1 and Γ_2 is such that a constant cross section A_2 is realized.

Based on the above statements, the optimization problem could be reduced to the 2D problem of finding the shapes of the two contours Γ_1 and Γ_2, which give a minimal overall volume and constant cross sectional areas of the solids S_1 and S_2.

2.2. Definition of the optimization problem

With the above discussed assumptions of cylindrical symmetry and mirror symmetry, the transformer geometry is fully described by the core contour Γ_1 separating the core from the windings, and the contour Γ_2 of the outermost winding being the visible shape of the transformer. Using these two contours, all quantities entering the volume characteristic (3) can now be formally expressed as follows:

$$A_1 = 2 \int_{\Gamma_1} z \, dr \, , \quad V = 4\pi \int_{\Gamma_2} zr \, dr \, , \quad A_2 = \pi = \text{const.} \tag{7}$$

Note that A_2 can be chosen constant since uniform scaling of the geometry does not change z_V at all. Furthermore, the choice $A_2 = \pi$ results in an innermost windings cross section with radius 1. The constancy of A_2 along the path l_2 introduces a constraint on the contours: the "distance" between them has to ensure the constant windings cross section A_2. As will be shown in the following, this constraint is so strong that for enough regular core shapes it provides a bijective relation between Γ_1 and Γ_2. This is intuitively clear if one imagines how the transformer core Γ_1 is gradually wrapped with windings until the final form Γ_2 results. Thus, Γ_1 enters the calculus as the only independent argument, all other objects, i.e., A_1, Γ_2 and V follow from it. This allows us to define the optimization problem as follows:

> Find a contour Γ_1 of the iron core which minimizes z_V according to Equations (3) and (7) and under the constraint $A_2 = \pi = \text{const.}$

2.3. The relation between the contours

Intuitively the existence of a relation between the shape of the core Γ_1 and the shape of the outermost winding Γ_2 is apparent: the final design is obtained by the successive coating of the initially bare core with infinitesimal layers of windings with constant cross-section, so a constant current density can be realized. In principle, this process can be directly simulated. However, such a numerical procedure was shown to be time consuming and prone to the accumulation of considerable errors, especially for less regular core geometries, which tend to appear during the numerical optimization of Γ_1. Thus, it is desirable to have a robust and fast algorithm that assigns Γ_2 to Γ_1. There is an analytical approach to this problem, and it requires the detailed analysis of the current density in the windings section S_2. The current density is a vector field $\mathbf{J} : \mathbb{R}^3 \to \mathbb{R}^3$ with the following properties:

1. Due to cylindrical and reflection symmetry, $\mathbf{J}$ only depends on the coordinates r and z and the azimuthal component of $\mathbf{J}$ is assumed to vanish. This reads as $\mathbf{J} : (r, z) \to (J_r, J_z)$.
2. Since the maximum admissible current density should be achieved everywhere, $\mathbf{J}$ has a constant norm, i.e., $\|\mathbf{J}\| = J = \text{const.}$ Thus, $J_r = J \cos(\alpha)$ and $J_z = J \sin(\alpha)$ and the remaining unknown is the orientation field $\alpha : (r, z) \to \alpha$.
3. The current is quasi-static, thus $\mathbf{J}$ has zero divergence since charge must not accumulate anywhere [1]. This reads as $\text{div}(\mathbf{J}) = 0$, or in cylindrical coordinates $\frac{1}{r}\frac{\partial}{\partial r}(rJ_r) + \frac{\partial}{\partial z}J_z = 0$.

By substituting step 2 into step 3 and crossing out the current norm J, a partial differential equation (PDE) for the scalar orientation field $\alpha(r, z)$ is obtained, which is quasilinear, inhomogeneous and hyperbolic [8]. It can be written in the form of a scalar product:

$$\begin{pmatrix} -\sin(\alpha) \\ \cos(\alpha) \end{pmatrix} \cdot \begin{pmatrix} \partial\alpha/\partial r \\ \partial\alpha/\partial z \end{pmatrix} = -\frac{1}{r}\cos(\alpha) \tag{8}$$

The projection of the gradient of α onto the normal $\mathbf{n} = (-\sin(\alpha), \cos(\alpha))^{\mathrm{T}}$ to the windings equals $-\frac{1}{r}\cos(\alpha)$, so we know the rate of change of α along direction $\mathbf{n}$, cf. Figure 6. At the same time α determines $\mathbf{n}$. Thus, it is possible to calculate the field α on a slice in the rz-plane by integrating $d\alpha = -\frac{1}{r}\cos(\alpha)ds$ along the trajectory ϑ, which arises from the subsequent vectorial addition of line elements $\mathbf{n} \, ds$. In terms of techniques applied for the solution of hyperbolic partial differential equations, this is the so-called method of characteristics [9], and the characteristic here is the trajectory ϑ.
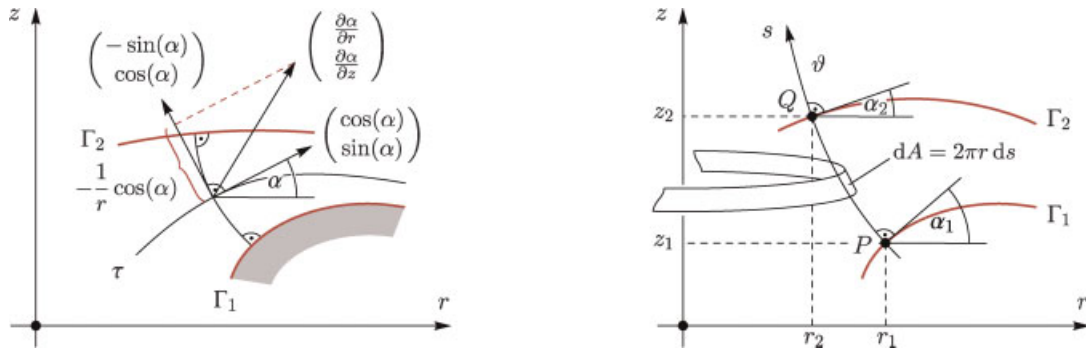
Figure 6. The geometry of the hyperbolic PDE (8). τ denotes a winding with orientation α, and ϑ the characteristic crossing τ at right angle. Since the cross-section A_2 is everywhere perpendicular to τ, $dA = 2\pi r ds$ holds.

The parameter s is the arc length along ϑ and if the dot denotes differentiation with respect to s according to $\dot{f} = df/ds$, the system of ordinary differential equations (ODE) to be solved is:

$$\vartheta : \quad \begin{pmatrix} \dot{\alpha} \\ \dot{r} \\ \dot{z} \end{pmatrix} = \begin{pmatrix} -\frac{1}{r}\cos(\alpha) \\ -\sin(\alpha) \\ \cos(\alpha) \end{pmatrix}, \quad \begin{pmatrix} \alpha(0) \\ r(0) \\ z(0) \end{pmatrix} = \begin{pmatrix} \alpha_1 \\ r_1 \\ z_1 \end{pmatrix} \tag{9}$$

The initial conditions at $s = 0$ were chosen such that the characteristic ϑ starts on the contour Γ_1 in the point $P = (r_1, z_1)$ where the windings orientation is α_1. After a solution for ϑ has been obtained, it is simple to determine the point $Q = (r_2, z_2)$ where ϑ crosses Γ_2. The windings area must integrate to A_2 and an increment in cross-section is given by $dA = 2\pi r ds$, cf. Figure 6. Thus, the arc length s_2 at which ϑ crosses Γ_2 is implicitly given by solving the following problem for s_2:

$$\dot{A} = 2\pi r, \quad A(0) = 0, \quad A(s_2) = A_2 \tag{10}$$

If s_2 is known, the coordinates $r_2 = r(s_2)$ and $z_2 = z(s_2)$ become accessible and the point Q is an element of the contour Γ_2. So a mathematical formulation for the mapping $\Gamma_1 \rightarrow \Gamma_2$ was found.

2.4. An efficient algorithm

There is a simpler way to do the assignment $(r_1, z_1, \alpha_1) \rightarrow (r_2, z_2)$ than by solving the four coupled ODEs (9) and (10) for s_2. It is possible to find an analytical expression for the characteristic ϑ in terms of an explicit dependence $z \rightarrow r$. The characteristic in the representation $r(z)$ fulfills a nonlinear second order differential equation which is equivalent to (9) but omits the use of arc length. By differentiating the second and third equation of (9) with respect to s, $\ddot{r} = \dot{z}^2/r$ and $\ddot{z} = -\dot{r}\dot{z}/r$ are obtained. Furthermore, if the prime denotes differentiation with respect to z according to $f' = df/dz$, the chain rule of differentiation gives $\dot{r} = r'\dot{z}$ and $\ddot{r} = r''\dot{z}^2 + r'\ddot{z}$. After eliminating $\ddot{r}$, $\ddot{z}$, and $\dot{r}$ from these four statements, the factor $\dot{z}^2$ cancels and the remaining differential equation for $r(z)$ equipped with the proper initial conditions reads as

$$\vartheta : \quad rr'' = 1 + r'^2, \quad r(z_1) = r_1, \quad r'(z_1) = -\tan(\alpha_1) = v_1 \tag{11}$$

The general solution of this differential equation can be easily guessed. First, it is obvious that the hyperbolic cosine $r(z) = \cosh(z)$ fulfills the equation. Second, no characteristic length scale enters the equation. This means an isotropic scaling of the solution must be again a solution, thus the first of the two expected integration constants should provide this scaling. And third, the equation is cyclic in z, i.e., z doesn't appear explicitly. This means a translation of the solution in the z-direction is again a solution, thus the

second of the two integration constants should provide this translation. By choosing these two integration constants C_1 and C_2 properly, the general solution satisfying the initial value problem (11) is given by:

$$r(z) = C_1 \cosh\left(\frac{z - C_2}{C_1}\right) , \quad C_1 = \frac{r_1}{\sqrt{1 + v_1^2}} , \quad C_2 = z_1 - r_1 \frac{\text{asinh}(v_1)}{\sqrt{1 + v_1^2}} \tag{12}$$

A reformulation of Equation (10) allows to derive a relation for the location of the point Q. By realizing that $A' = 2\pi r\sqrt{1 + r'^2}$, substituting (12) in A', integrating from z_1 to z_2 and setting this result equal to A_2, a transcendental equation for z_2 is obtained:

$$A_2 = \text{sig}(\cos(\alpha_1))\pi C_1^2 \cdot \left[\frac{1}{2}\sinh\left(\frac{2(z_2 - C_2)}{C_1}\right) - \frac{1}{2}\sinh\left(\frac{2(z_1 - C_2)}{C_1}\right) + \frac{z_2 - z_1}{C_1}\right] \tag{13}$$

Here sig(.) denotes the signum function, which fixes the sign of the integral such that the positivity of area A_2 is ensured, no matter in which direction the integration is performed. The cases $\alpha_1 = \pi/2 + n\pi$, $n \in \mathbb{Z}$ have to be treated separately due to the appearance of poles in v_1, see (11). In this case the characteristics are $z = \text{const.}$, and so $z_2 = z_1$ and $r_2 = \sqrt{r_1^2 - \text{sig}(\sin(\alpha_1))A_2/\pi}$. Now the algorithm for the calculation of the contour Γ_2 is the following:

1. Choose on Γ_1 enough points $P^i = (r_1^i, z_1^i)$, $i = 1, \dots, N$, including the local orientation α_1^i;
2. For all points solve (13) for z_2; and
3. Determine r_2 by using Equation (12).

Thus, to every point P^i on Γ_1 a point $Q^i = (r_2^i, z_2^i)$ on Γ_2 is assigned such that the contours enclose the area A_2. The step 2 involves the solution of the transcendental Equation (13) for z_2. This is best carried out numerically with a Newton–Raphson algorithm. By vectorizing the algorithm, a very fast and robust assignment $\Gamma_1 \rightarrow \Gamma_2$ can be realized.

2.5. Discretized representation of the geometry

Before the optimization of the volume characteristic can be started, a formal definition of the core contour Γ_1 is necessary, which can be done by an explicit assignment $r \rightarrow z$ or a parametrized form $s \rightarrow (r, z)$. Particular choices of such parametrizations of Γ_1 will be presented in the following. However, at this point the qualitative outcome of the optimization must be anticipated in order to justify the features introduced in the modeling of Γ_1.

Namely, it is observed that the core shape—if subject to the minimization of z_V—behaves like a waterdrop lying on a horizontal, plane and hydrophobic surface which is parallel to the z-axis. The waterdrop wants to become as flat as possible in order to minimize its gravitational potential energy by lowering its center of mass. But at the same time it tries to retain a spherical shape in order to minimize the surface energy at constant volume. The outcome of these competing tendencies is a compromise: an elliptic-like shape, which is oblate at the point where the waterdrop is in contact with the surface.

The analogies with the transformer optimization presented here are as follows (refer to Equations (1), (3), and Figure 7). The region enclosed by Γ_1 is the waterdrop, A_1 is its ''volume'' and the mean length l_2 of the windings its ''surface''. The gravitational effect is generated by the cylindrical geometry, which favors cores with short mean lengths l_1, thus pulls the shape toward the z-axis. And the effect of the surface energy is represented in the favoring of windings with short lengths l_2, thus driving Γ_1 toward a circle.

Indeed, the best optimization results are obtained if Γ_1 is given the shape of a waterdrop ''sitting'' at distance 1 above the z-axis. Several techniques realizing a corresponding discretization were tested. Of all these approaches the two associated with the most accurate results in z_V are presented here.

2.5.1. Representation with local Bézier segments. With this method, $N+1$ points P^i, $i = 0, \dots, N$ with assigned fixed orientations $\alpha_1^i = \pi(1/2 - i/N)$ are chosen on Γ_1. Two neighboring points P^i and P^{i+1} are connected by quadratic Bézier segments [10] defined by the three control points $P^i = (r_1^i, z_1^i)$, $B^i = (r_B^i, z_B^i)$, and $P^{i+1} = (r_1^{i+1}, z_1^{i+1})$ where B^i is the intersection of the tangents at P^i and P^{i+1}, cf. Figure 7 left. If a local parameter $t \in [0, 1]$ is introduced, the parametrized representation of one such Bézier segment is given as:

$$\begin{pmatrix} r_1(t) \\ z_1(t) \end{pmatrix} = \left(\begin{pmatrix} r_1^i \\ z_1^i \end{pmatrix} - 2\begin{pmatrix} r_B^i \\ z_B^i \end{pmatrix} + \begin{pmatrix} r_1^{i+1} \\ z_1^{i+1} \end{pmatrix}\right)t^2 + 2\left(\begin{pmatrix} r_B^i \\ z_B^i \end{pmatrix} - \begin{pmatrix} r_1^i \\ z_1^i \end{pmatrix}\right)t + \begin{pmatrix} r_1^i \\ z_1^i \end{pmatrix} \tag{14}$$
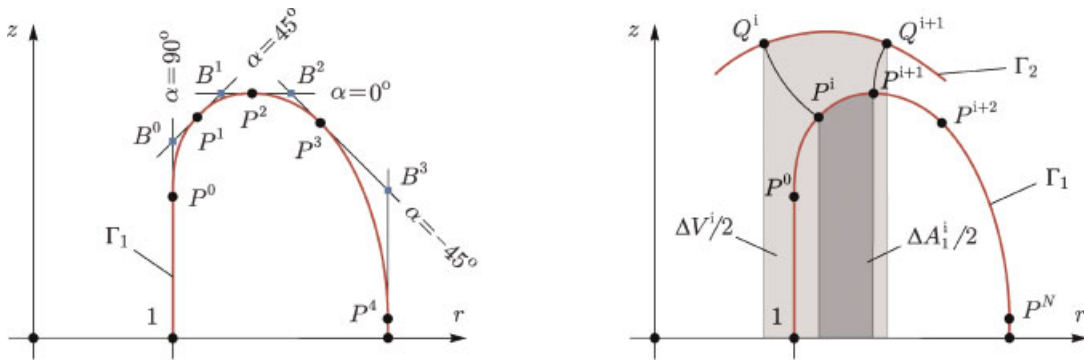
Figure 7. Left: representation of the core contour by Bézier curve segments for $N = 4$. Right: contributions of the ith segment to the core cross-section A_1 and the total volume V.

The discrete degrees of freedom left free for the optimization are the coordinates (r_1^i, z_1^i) of every point P^i with exception of $r_1^0 = 1$. If z_1 takes positive values at the boundaries, i.e., $z_1^0 > 0$ and/or $z_1^N > 0$, then vertical line segments are added to the core contour. The union of Bézier and vertical line segments is a smooth curve representing a valid core contour. The contribution ΔA_1^i of segment according to (14) to the area A_1 is given as follows, compare with Equation (7):

$$\Delta A_1^i = 2 \int_0^1 z(t)\dot{r}(t)\,\mathrm{d}t = \frac{(3r_1^{i+1} - r_1^i)z_1^{i+1} - (3r_1^i - r_1^{i+1})z_1^i}{3} + \frac{2(r_1^{i+1} - r_1^i)z_B^i - 2r_B^i(z_1^{i+1} - z_1^i)}{3} \tag{15}$$

The contribution ΔV^i of this segment to the total volume V needs to be computed numerically. For this purpose, more sample points on the core contour are obtained from Equation (14) and the corresponding points on the windings contour by the numerical procedure described in Section 2.4. The orientation of the windings contour at these points is calculated with Equation (11) and used for the construction of cubic Hermite splines connecting two neighboring points. The volume integral contribution is then analytically evaluated with Hermite interpolation. An advantage of this discretization is its locality. If a discretization point P^i is moved during the optimization, only the contributions of two neighboring curve segments to the core cross-section A_1 and the total volume V need to be updated, cf. Figure 7 right. This is especially important if the efficient calculation of the Jacobian is required.

2.5.2. Representation by superposed nonlocal functions. In this method, the core contour is realized by the superposition of several nonlocal basis functions and every basis function is parametrized by the same global parameter $t \in [0, \pi]$. In order to realize the waterdrop-like shape, three types of basis functions are superposed: a triangle, an ellipse, and several Fourier modes [11], cf. Figure 8. The mathematical definition of the so obtained core contour except the vertical line segment is:

$$\begin{pmatrix} r_1(t) \\ z_1(t) \end{pmatrix} = \begin{pmatrix} 1 + a(1 - \cos(t)) \\ b\sin(t) + \frac{c}{2}(1 + \cos(t)) + \sum_{k=1}^{n} f_k \sin\left(\frac{k\pi}{2a}(r_1(t) - 1)\right) \end{pmatrix} \tag{16}$$
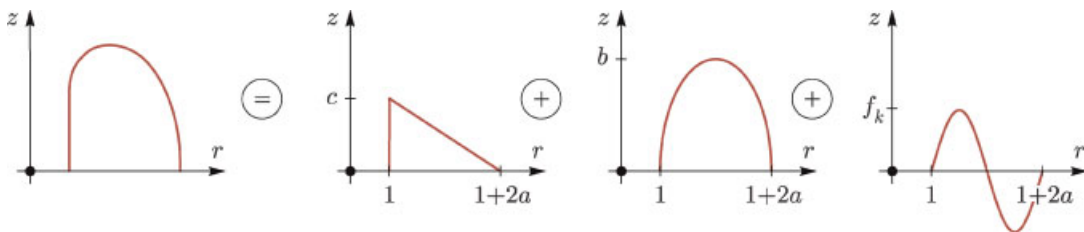
Figure 8. Representation of the core contour by superposition of global basis functions: triangle, ellipse, and Fourier modes.

The discrete degrees of freedom are the semi-minor axis a, the semi-major axis b, the vertical line segment c and the n Fourier coefficients f_k, $k = 1, \ldots, n$. Unlike in the case of Bézier segments, where the orientation α_1 was fixed a priori, the representation (16) determines the orientation according to $\alpha_1 = \arg(\dot{r}_1 + i\, \dot{z}_1)$, where i is the imaginary unit. For the computation of the windings contour and the integration of A_1 and V, dense grids of points P^i on Γ_1 and the assigned points Q^i on Γ_2 are introduced. The integrals according to Equation (7) are approximated by using linear interpolations of Γ_1 and Γ_2 between adjacent points. The contributions of one segment to A_1 and V are then given by the equations:

$$\Delta A_1^i = \left(r_1^{i+1} - r_1^i\right)\left(z_1^{i+1} + z_1^i\right) \tag{17}$$

$$\Delta V^i = \frac{2\pi}{3}\left(r_2^{i+1} - r_2^i\right)\left(r_2^i z_2^i + r_2^{i+1} z_2^{i+1} + \left(r_2^{i+1} + r_2^i\right)\left(z_2^{i+1} + z_2^i\right)\right) \tag{18}$$

Compared to the previously discussed Bézier method, this discretization lacks locality. All basis functions have global support, thus the position and orientation of a point P^i is generally a function of all parameters a, b, c and the f_k, so all degrees of freedom are coupled. The advantage of this representation is the existence of the compact Equations (16) that allows the quick construction of Γ_1.

2.6. Numerical optimization

At this stage the initial problem of minimizing the volume characteristic z_V is recast into a form suitable for the numerical optimization. The incorporated simplifications were explained in Section 2.1, the minimization problem was defined in Section 2.2, the treatment of the constraint $A_2 = \pi = $ const. was analytically solved in Section 2.3, and a corresponding algorithm for the assignment $\Gamma_1 \to \Gamma_2$ was presented in Section 2.4. With the discretization of the core contour Γ_1 according to Section 2.5, the functional z_V now depends on a finite set of discrete degrees of freedom (or parameters) which describe the complete transformer geometry. An optimization algorithm can search for the parameter set which minimizes z_V.

For an efficient numerical optimization it is essential that the number of degrees of freedom can be refined dynamically. Starting with a coarse discretization, it is refined whenever z_V can no more be sufficiently improved. Refining the discretization should add degrees of freedom while keeping the represented curve initially unchanged. This requirement is met by both methods presented in Section 2.5. For instance, subdividing a Bézier segment does not change the curve if the new control points are properly defined. For this purpose all segments were simultaneously subdivided at the points on the curve where α_1 is an odd multiple of $\frac{\pi}{2N}$. These points can be computed analytically. With the nonlocal discretization method, the addition of Fourier modes does not change the former representation if the new Fourier coefficients are initially set to zero.

By optimizing the $2N + 1$ coordinates $z_0, r_1, z_1, \ldots, r_N, z_N$ or the $n + 3$ parameters a, b, c, $f_1, \ldots, f_n$, we obtained core contours minimizing the associated z_V. Depending on the type of discretization, different numerical methods were applied, i.e., Conjugate Gradients, Quasi Newton [12] and Steepest Descent with the Bézier discretization and the Nelder–Mead method [13] with the nonlocal discretization, respectively. In Table II the minimum value z_V is listed against the number of points P^i for the Bézier discretization and the three different minimization algorithms. All algorithms quickly converge to the same result and so consolidate the final minimum value $z_V = 10.07364287$ in average.

Table II. Convergence of z_V against the number of points P^i as obtained with the Bézier discretization and with different minimization algorithms.

Discretization points P^i $(N+1)$	Volume characteristic z_V		
	Conjugate Gradients NAG C library	Quasi Newton NAG C library	Steepest Descent C++
3	10.0809155	10.0802867	10.0802867
5	10.0737844	10.0737844	10.0737844
9	10.0736544	10.0736544	10.0736544
17	10.0736446	10.0736446	10.0736446
33	10.0736431	10.0736431	10.0736432
65	10.0736428	10.0736428	10.0736432
129	10.0736428	10.0736428	10.0736431
257	10.0736428	10.0736428	10.0736430

Table III. Convergence of z_V against the number of integration nodes as obtained with the nonlocal discretization (16 Fourier modes) and with the Nelder–Mead search algorithm.

Nodes	a	b	c	z_V
114	0.56544160	0.92664917	0.34566179	10.07351972
229	0.56540864	0.93020924	0.34475896	10.07362431
457	0.56540084	0.93104536	0.34454213	10.07364997
914	0.56539894	0.93124732	0.34448906	10.07365633
1829	0.56539850	0.93129277	0.34447670	10.07365791
3657	0.56539848	0.93129511	0.34447502	10.07365830
7314	0.56539850	0.93129717	0.34447417	10.07365840
14629	0.56539847	0.93129828	0.34447408	10.07365843

In Table III, the convergence analysis is listed for the nonlocal discretization and the Nelder–Mead minimization. The minimum value z_V together with the corresponding parameters a, b, and c are listed against the number of nodes introduced for the integration. All runs were realized with $n = 16$ Fourier modes, and increasing this number could not improve z_V. The final number $z_V = 10.07365843$ deviates in the fifth position after decimal point from the result obtained with the Bézier discretization, so the two methods differ by a negligible relative error of $1.5 \cdot 10^{-6}$.

Regarding Table III, one should become aware that increasing the number of nodes makes z_V become larger, which is due to the enhanced integration. It was generally observed that shortcomings in the modeling of the windings field and insufficient discretization tend to spuriously lower the minimum z_V, which makes it necessary to interpret minimization results very carefully.

Table IV. The geometrical parameters of the optimum design as obtained with the nonlocal discretization. Use equation (16) to plot the core contour.

$V =$ 36.94848302	$A_1 =$ 1.80051185	$A_2 =$ 3.14159265	$z_V = 10.07365843$
$a =$ 0.56539847	$b =$ 0.93129828	$c =$ 0.34447408	
$f_1 = -0.16321756$	$f_2 = -0.01650819$	$f_3 = -0.01360955$	$f_4 = -0.00288422$
$f_5 = -0.00400781$	$f_6 = -0.00077503$	$f_7 = -0.00167010$	$f_8 = -0.00022080$
$f_9 = -0.00080590$	$f_{10} = -0.00004639$	$f_{11} = -0.00041009$	$f_{12} = 0.00000631$
$f_{13} = -0.00020228$	$f_{14} = 0.00001346$	$f_{15} = -0.00008063$	$f_{16} = 0.00000129$
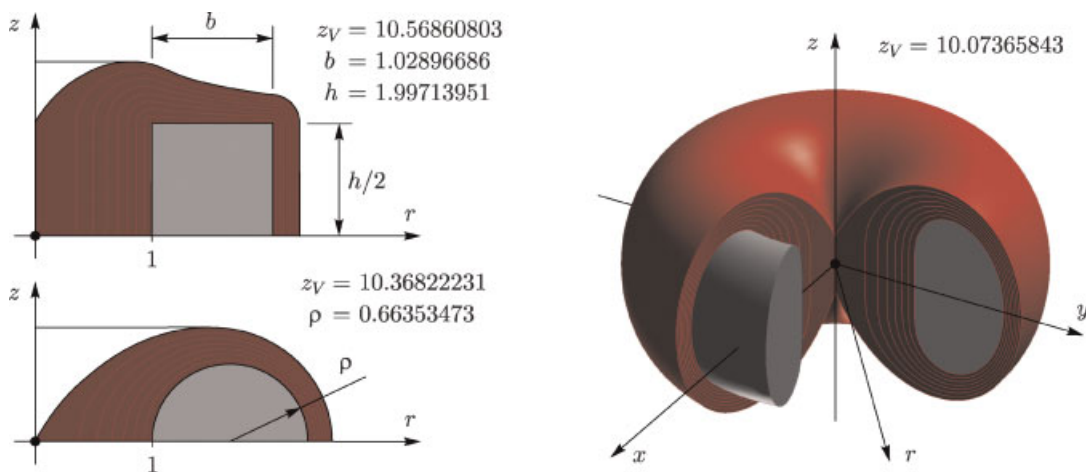
Figure 9. Left: cross sections of optimum rectangular and circular core shapes. Right: the rendered 3D representation of the optimum transformer geometry as obtained with the waterdrop-like core shape.

Finally, the geometric parameters corresponding to the optimum core shape are listed in Table IV. In Figure 9, the corresponding optimum geometry is visualized in 3D. In the same figure two simpler geometries are reported, i.e., a circular and a rectangular core shape. These shapes are described by few parameters and can be easily manufactured. The parameters were optimized with the same methods reported above. However, with these simple contours it is not possible to bring the volume characteristic down to the value obtained with the waterdrop-like shape.

3. CONCLUSION

3.1. Summary and discussion

With numerical optimization techniques we computed the optimal core contour leading to a transformer geometry with a minimum volume characteristic $z_V = 10.07365 \pm 10^{-5}$. Arguments were given, why the optimum geometry should have the rotational and reflection symmetry, which considerably reduced the complexity of the task. A constrained minimization problem was defined, where the constraint emanates from the requirement of a constant cross-sectional area of the transformer windings. The constraint was resolved using the theoretical framework of hyperbolic partial differential equations, and the method of characteristics was used for solving the field equation for the windings orientation. An analytical formula could be derived, relating the core and windings contour. Finally, different discretization and solution procedures were applied in the numerical search of the optimal design and the results of the various methods were found to be in excellent agreement.

Being the solution of a variational problem, the result is a local but not necessarily a global optimum. Our theoretical and numerical experiments suggest that this local optimum is unique within a wide parameter range, if not globally. However, we did not give a mathematically rigorous proof of global optimality, e.g., by proving the convexity of the functional to be optimized. Similarly, we gave no hard proofs for the assumption that the optimal core has a convex contour and cylindrical and reflection symmetry. Nevertheless, we believe that even by relaxing these constraints, it is not possible to obtain a design with a better volume characteristic.

3.2. Outlook

The here presented solution of the optimization problem takes advantage of the various simplifications as introduced in Section 2.1. It would be an interesting task to investigate the topic under more realistic and thus less strict assumptions, which however makes the problem more difficult to solve and introduces new parameters.

A first worthwhile step toward more realism would be to allow for an inhomogeneous magnetic flux density norm in the core. This step requires a physical solution for the magnetic field, a reconsideration of the power formula (2) and the setup of a new objective function (3). Going further and considering heating-up of the device, it would be necessary to solve a heat conduction problem on the trial geometry, which would considerably increase the complexity. Such extensions of the optimization problem have no impact on the assignment between core and windings contours according to Equation (13), thus the here presented strategies may be directly employed within such extended approaches. An open field, however, is the application and extension of the here presented ideas to involved geometries in 3D, having probably different topological properties than the here considered toroidal design.

Considering pure theory, two main issues remain. One is the still not satisfyingly answered question whether an optimizing geometry can be found within the discussed class of toroidal, symmetric designs as proposed and motivated in Section 2.1. A first improvement would be, if a stronger statement than Section 2.1.3 on the admissibility of cylindrical symmetry could be found. The second interesting open question is, whether the optimal geometry or the minimum of z_V can be expressed analytically. It seems unlikely that an analytic expression can be derived from our optimization techniques, so we did not explore this track further. Therefore, our optimal geometry can only be represented in its numerical discretization with either Bézier segments, Fourier series, or a similar method. It would be a challenging task to investigate the here presented optimization problem under a purely mathematical viewpoint and answer the question of analytical expressibility of z_V.

4. LIST OF SYMBOLS AND ABBREVIATIONS

4.1. Symbols

a, b, c, f_i geometrical parameters specifying the transformer geometry
α windings orientation field

A_1, A_2, A	cross sections of the core and windings, windings area function
B	magnetic flux density norm
C_1, C_2	integration constants
$\mathcal{D}_S, \mathcal{D}_N$	particular symmetric and nonsymmetric transformer designs
ε	perturbation parameter
Φ	total magnetic flux
Γ_1, Γ_2	contours of the core and windings in the first quadrant of the rz-plane
I	total current
$\mathbf{J}, J, J_r, J_z$	current density vector, its norm, r- and z-components
k	overall utilization factor
l_1, l_2	mean lengths of the core and windings
$\mathbf{n}$	normal vector orthogonal to the windings
N, n	integer numbers referring to the degree of discretization
ω	angular frequency
P, P^i	particular point or several points on the core contour
Ψ, Φ	partition functions
Q, Q^i	particular point or several points on the windings contour
r, φ	radius and angle of the polar parametrization of the xy-plane
$\mathcal{R}$	rule assigning symmetric to nonsymmetric designs
$\mathbb{R}, \mathbb{R}^3$	set of real numbers, 3D space of real numbers
s	arc length along a characteristic
S_1, S_2	solids of magnetically and electrically conductive material
$\mathcal{S}$	geometrical symmetry
$\mathcal{T}$	set of transformer designs
$\mathcal{T}_S, \mathcal{T}_N$	subsets of symmetric and nonsymmetric transformer designs
τ	symbol for a winding
ϑ	symbol for the characteristic crossing windings at right angle
V_1, V_2, V	volumes of the core and windings, total transformer volume
x, y, z	axes of an orthogonal Cartesian coordinate system
z_V, z_W	volume and weight characteristics
$\mathbb{Z}$	set of integer numbers

4.2. Abbrevations

2D, 3D	two-dimensional and three-dimensional
ABB	Asea Brown Boveri
NAG	Numerical Algorithms Group
ODE	ordinary differential equation
PDE	partial differential equation

REFERENCES

1. Jackson JD. *Classical Electrodynamics*, 3rd edn. John Wiley & Sons Inc.: New York, 1998; ISBN 0-471-30932-X.
2. Gärtner R. Designing principles for transformers 1. The ring transformer (in German). *Archiv für Elektrotechnik* 1980; **62**(4–5):187–194.
3. Di Barba P, Kladas A, Neittaanmäki P, Rudnicki M, Savini A. Application of global optimization strategies to the shape design of a transformer winding. *Advances in Engineering Software* 1994; **19**(2):121–125.

4. Hurley WG, Wölfle WH, Breslin JG. Optimized transformer design: inclusive of high-frequency effects. *IEEE Transactions on Power Electronics* 1998; **13**(4):651–659.
5. Byun JK, Hahn SY, Park IH. Topology optimization of electrical devices using mutual energy and sensitivity. *IEEE Transactions on Magnetics* 1999; **35**(5):3718–3720.
6. Georgilakis PS, Tsili MA, Souflaris AT. A heuristic solution to the transformer manufacturing cost optimization problem. *Journal of Materials Processing Technology* 2007; **181**(1–3):260–266.
7. Courant R, Hilbert D. *Methoden der mathematischen Physik*. Springer Verlag: Vierte Auflage, Berlin, 1993; ISBN 3-540-56796-8.
8. Hungerbühler N. *Einführung in Partielle Differentialgleichungen*. vdf Hochschulverlag AG: Zürich, 1997; ISBN 3-7281-2303 -X.
9. Zwillinger D. *Handbook of Differential Equations*, 3rd edn. Academic Press: New York, 1997; ISBN 0-127-84396-5.
10. Bartels RH, Beatty JC, Barsky BA. *An Introduction to Splines for Use in Computer Graphics and Geometric Modeling*, 1st edn. Morgan Kaufmann Publishers Inc.: Los Altos, 1995; ISBN 1-558-60400-6.
11. James G. *Advanced Modern Engineering Mathematics*, 2nd edn. Addison–Wesley: New York, 1999; ISBN 0-201-59621-0.
12. Numerical Algorithms Group Ltd. *The NAG C Library Manual, Mark* 7. Oxford, December 2002, ISBN 1-85206-201-0, http://www.nag.co.uk
13. Nelder JA, Mead R. A simplex-method for function minimization. *Computer Journal* 1965; **7**(4):308–313.